J. Phys. Chem. A **2004,** *108,* 11419−11432

Theoretical Investigations of Acetylcholine (ACh) and Acetylthiocholine (ATCh) Using ab Initio and Effective Fragment Potential Methods

Jie Song and Mark S. Gordon*

Department of Chemistry, Iowa State University, Ames, Iowa 50011

Carol A. Deakyne

Department of Chemistry, University of Missouri—Columbia, Columbia, Missouri 65211

Wencui Zheng

Department of Chemistry, Eastern Illinois University, Charleston, Illinois 61920

Received: September 9, 2004

Both the effective fragment potential method and fully ab initio HF and MP2 methods have been used to study solvation effects on the conformational potential energy surfaces of ACh and ATCh. Comparisons of hydrated geometries and relative energies show that EFP1 can generate results quite close to the much more time-consuming ab initio calculations. Hydrated structures of ACh and ATCh prefer bridged water structures. Very limited effects from the solvation have been observed in ACh and ATCh. In both the gas and aqueous solution, ACh prefers the gauche NCCO arrangement, whereas ATCh favors trans NCCS. Possible interpretations are discussed.

I. Introduction

Acetylcholine, $CH_3CO_2CH_2CH_2N(CH_3)_3^+$ (ACh), is an important neurotransmitter in both the central and the peripheral nervous systems.[1] It was first discovered as the substance released by stimulation of the vagus nerve that alters heart muscle contractions.[2] ACh (Scheme 1) is produced by the synthetic enzyme choline acetyltransferase.[3−4] Upon release, ACh is metabolized into choline and acetate by acetylcholinesterase (AChE), and other nonspecific esterases. The binding mechanism has been of interest for many years. Recent studies[2−3,5−6] have shown that ACh traverses a deep groove lined with aromatic acids after leaving the aqueous environment of the synaptic cleft and before reaching the active site in AChE. Combined with up to three water molecules, some aromatic residues may also bind to the choline end of ACh in the active site. It has been proposed that such residues existing in the ACh receptor channel may be involved in cation−π interactions, which can assist the desolvation of the cation and provide ion selectivity.[2,7−9] Since the bonding is too weak to trap ACh, this allows its transit to the more strongly bonding receptor sites.

To describe the binding mechanism, and therefore its biological activity, it is important to understand the conformations of ACh and the possible changes in conformations in solvent (i.e., water). The conformational analysis of ACh has been the subject of many experimental[10−29] and theoretical[30−52] investigations. The different conformations of ACh can be derived from the rotation of the four internal torsional angles,[49] $C_4N_1C_5C_6$, $N_1C_5C_6O_7$, $C_5C_6O_7C_8$, and $C_6O_7C_8C_{10}$ (Scheme 1). Two of these, $C_4N_1C_5C_6$ and $C_6O_7C_8C_{10}$, are found to be trans in most of the previous experimental and theoretical studies.[11−13,30−32,38−41] The remaining torsions $N_1C_5C_6O_7$ and $C_5C_6O_7C_8$ are used to describe the conformational flexibility of ACh. In the gas phase, each of these rotation angles can be trans (*t*, ∼180°), gauche (g, ∼120°), or gauche′ (g′, ∼ −120°).

SCHEME 1. ACh and ATCh

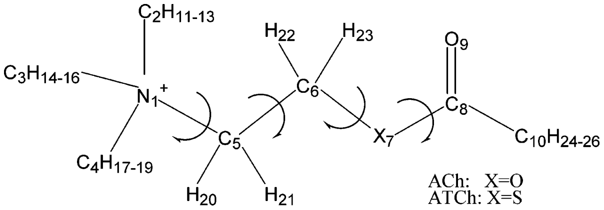

Aspects of the ACh potential energy surface (PES) have been the subject of numerous experimental investigations, including X-ray,[10−12,20−25] NMR,[13,15−18,27,29] electron diffraction,[26] and Raman spectroscopy.[19] Computational studies have employed ab initio,[2,35,38−39,48−50] semiempirical, and empirical methods,[30−34,42−45] as well as molecular dynamics.[40−41,52] However, despite the large number of reported works, several issues remain unresolved. Experiment and computations provide evidence of the high flexibility of ACh, as well as the possible existence of different conformations very close in energy. In addition to studying the conformations of ACh in the gas phase, it is also important to investigate environmental effects, presumably, via hydrogen bonds. These solvent effects may be systematically studied by adding explicit water molecules in a “supermolecule” or cluster approach.

One of the authors has previously studied the five possible gas phase conformations, gg′, gg, gt, tg, and tt, using Hartree−Fock (HF) with the 6-31G(d) basis set.[2] In this notation, the first and second letters refer to the $N_1C_5C_6O_7$ and $C_5C_6O_7C_8$ dihedral angles, respectively. The gg′ conformation was predicted to be the most stable rotamer. The strengths of interactions between an ion, such as ACh, and surrounding solvent molecules are important in computational modeling,[2] and the interactions between ACh and water may be competitive in stability with those between ACh and aromatic groups. Hence hydrated ACh

10.1021/jp0406013 CCC: $27.50

with one or two water molecules was also studied in the previous work.[2] Both conventional and unconventional hydrogen bonds, e.g., C−H···O, may be involved in the intramolecular and intermolecular solvation of ACh. Several stable HF/6-31G(d) hydrated structures have been predicted, and the hydrated gt conformations were found to be most stable, in the presence of one or two waters, in agreement with solution NMR studies.[15] It was suggested that the change in ACh conformation relative to the gas-phase enhances the formation of stronger bonding with water molecules.

Considerably less attention has been paid to the sulfur analogue acetylthiocholine (ATCh), although ACh and ATCh are assumed to have essentially identical kinetic properties with respect to acetylcholinesterase.[53] ATCh is often used as the substrate rather than ACh because it is easier to assay. Since S is less electronegative than O, ACh is expected to have stronger intramolecular hydrogen bonds (and stronger electrostatic interactions) than ATCh. Clearly, a systematic analysis of ATCh and its hydrated structures is of interest, given the important role of sulfur-containing compounds in biology and biochemistry.

In this study, the effects of n water molecules ($n = 1, 2, 3$) on the conformational PES of ACh and ATCh are studied, using both the effective fragment potential method[54,55] and fully ab initio calculations at a higher level than previously employed. The possible binding mechanisms of ACh and ATCh and the differences between them are discussed. The EFP method is briefly summarized in section II, and the computational details are described in section III. The results and discussion are presented in section IV. A final summary section concludes the paper.

II. EFP1/HF Method

The EFP1/HF method[54,55] has proved to be effective for treating aqueous solvation. It can provide quantatively correct results compared to the HF method with considerably lower computational costs. The EFP method has been described in detail elsewhere, so its features will only be briefly summarized here. The model treats each solvent molecule explicitly, by adding one-electron terms directly to the ab initio Hamiltonian,

$$H_{\mathrm{TOT}} = H_{\mathrm{AR}} + V \tag{1}$$

The "active region" (AR) contains the solute and any solvent molecules directly involved in a bond forming/breaking process. The AR is explicitly treated with the ab initio wave function of choice. The remainder of the system is represented as a sum of effective fragment potentials V. There are three one-electron terms in V at the HF level: (1) Coulombic interactions between solvent molecules (fragment−fragment) and solvent molecules with ab initio solute molecules (fragment−ab initio), including a charge penetration correction to account for overlapping electron densities; (2) self-consistent polarization interaction between solvent molecules (fragment−fragment) and solvent molecules with ab initio solute molecules (fragment−ab initio); (3) exchange repulsion, and charge transfer. The contributions from the first two terms are determined based on the properties of the water monomer calculated using ab initio methods. The last term is determined by a fitting procedure to the ab initio potential of the water dimer. For the μth solvent molecule, the effective fragment potential interaction with the solute is given by

$$V_{\mathrm{el}}(\mu,s) = \sum_{k=1}^{K} V_k^{\mathrm{elec}}(\mu, s) + \sum_{l=1}^{L} V_l^{\mathrm{pol}}(\mu, s) + \sum_{m=1}^{M} V_m^{\mathrm{Rep}}(\mu, s) \tag{2}$$

where s is the nuclear coordinate; k, l, and m are the number of expansion points for Coulombic, polarization, and exchange repulsion interactions, respectively. For the water molecule, K, L, and M are equal to 5 (nuclear centers and bond midpoints), 5 (bonding lone-pair and inner shell localized molecular orbitals), and 4 (fragment atom centers and center of mass), respectively.

Although there is no restriction on the ab initio level of theory in the AR part, the most consistent approach is to use the same level as that used to derive the EFP. The internal geometry for each EFP is held fixed, although the EFP waters are allowed to independently translate and rotate as units during geometry optimizations. All calculations described in this work were performed using the electronic structure code GAMESS,[56] and geometries are viewed using MacMolPlt.[57]

III. Computational Details

Fully optimized structures of ACh, ACh(H_2O), and ACh(H_2O)$_2$ were computed at the HF/6-31G(d) level using the GAMESS electronic structure package. A large number of equilibrium structures were located and characterized as minima by a harmonic normal-mode analysis. The HF/6-31G(d) potential energy surfaces were found to be quite shallow. Zero-point energy corrections were applied to the molecules under study at the HF and second-order perturbation theory (MP2) levels (using HF/6-31G(d) optimized geometries). Selected structures with very similar predicted stabilities were reoptimized at the MP2/6-31G(d) level. The analogous calculations were repeated at the EFP1/HF level, treating the water molecules as effective fragments. Direct comparisons are made between the HF/6-31G(d) and EFP1/HF/6-31G(d) results. The same approaches were applied to ATCh, ATCh(H_2O), and ATCh(H_2O)$_2$. Finally, the hydrated ACh and ATCh structures with three water molecules were predicted at the EFP1/HF/6-31G(d) level.

The criteria used to define the existence of hydrogen bonds were chosen from ref 2: An H···O distance less than 2.8 Å and a C−H···O bond angle greater than 90°. These criteria are consistent with the ranges cited by Desiraju[58] and Steiner and Saenger.[59] However, the van der Waals radius of the oxygen atom is only 0.73 Å whereas that of the sulfur atom is 1.02 Å.[60] Therefore, the maximum allowed H···S distance is adjusted to 3.2 Å in the case of ATCh.

IV. Results and Discussions

Three possible interactions between water and ACh or ATCh are considered in this study (see schemes for labels): (1) between the carbonyl oxygen and a water hydroxyl group, O−H···O═C; (2) between the water oxygen and one or more quaternary (qa) methyl or methylene groups, C−H···O−H; (3) between the ACh ester oxygen or ATCh thioester sulfur and a water hydroxyl group[2] X···H−O (Scheme 2). Interactions involving acetoxy methyl groups ($C_{10}H_{24-26}$) are not considered due to their lower stability.[2,61−63] The label "br" is used to describe an O−H···O═C interaction if a water bridge is formed between the carbonyl oxygen and a quaternary methyl or methylene group (Scheme 3). When multiple water molecules are involved, it is possible to have a water bridge containing

SCHEME 2. Three Possible Water−ACh/ATCh Interactions

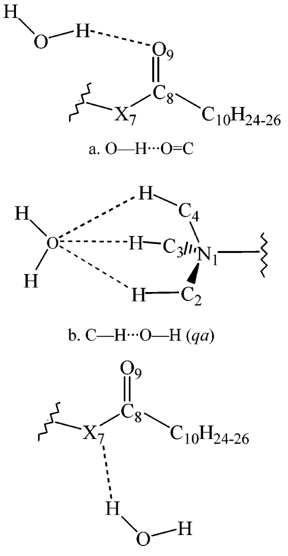

a. O—H···O=C

b. C—H···O—H (*qa*)

c. X···H—O

SCHEME 3. Three Water−Bridge Structures

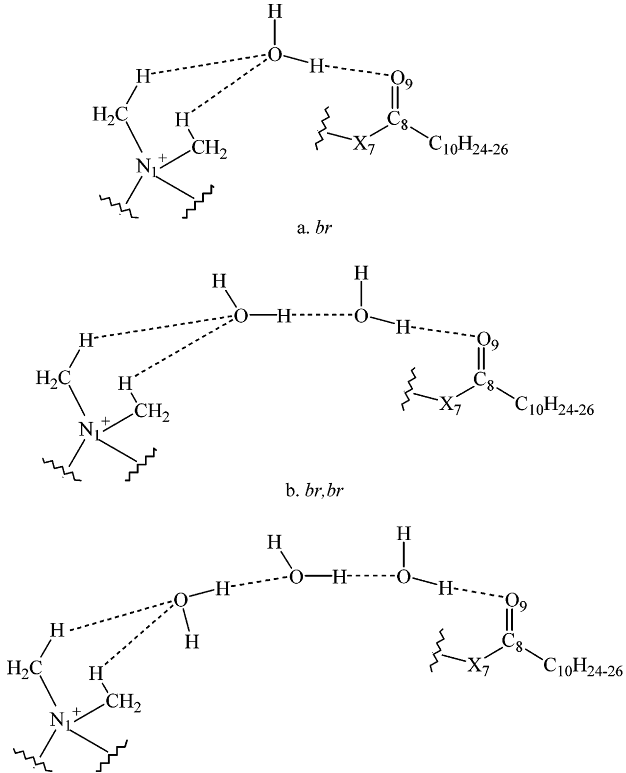

a. *br*

b. *br,br*

c. *br,br,br*

several waters. For example, “br, br” and “br, br, br” represent two-water and three-water bridges, respectively. The second type of interaction “qa” only occurs between a single water molecule and the quaternary methyl or methylene groups. The label “w” represents an interaction between a water oxygen atom and a hydroxyl group from another water. Since a “w” interaction always involves either a “br” or “qa” structure, the appropriate notation will be “qa, w” or “br, w”. Notations for a complex start from the name of the complex, either ACh or ATCh with no water, followed by the type of rotamer, and finally the arrangement of the water molecule(s). The water molecules are indicated in the same sequence as they appear and in accordance with the numbering scheme for the waters ($H_{28}O_{27}H_{29}$, $H_{31}O_{30}H_{32}$, and $H_{34}O_{33}H_{35}$ for the first, second, and third water molecule, respectively). With these abbreviations in mind, ACh(H_2O)$_3$, gt, br, w, qa may be interpreted as the gt rotamer of ACh with three water molecules: the first water molecule forms a one-water bridge, the second water has a “w” interaction with the first water, and the third water has an interaction with quaternary methyl or methylene groups. ACh(H_2O)$_3$, tt, qa, qa, w indicates a complex with the tt rotamer of ACh in which each of the first two water molecules form interactions with quaternary methyl or methylene groups and the third water forms a w interaction with the second one. ATCh(H_2O)$_3$ with the tg rotamer and a three-water bridge would be represented as ATCh(H_2O)$_3$, tg, br, br, br.

1. ACh, Gas Phase. Previous studies[2] showed that there are five conformations, gg′, gg, gt, tg, and tt (Figure 1), for ACh. Since the dihedral angles $C_4N_1C_5C_6$ and $C_6O_7C_8C_{10}$ are expected to be ∼180°, those are omitted from the tables, even though they are fully optimized. The calculations reported in this work (see Tables 1 and 2) reproduce the previous ab initio geometries.[2] Internal C- -H···O hydrogen bonds are found in four of the five conformers with the tt conformation being the exception. Intramolecular hydrogen bonds are observed (see Table 2) between the ester oxygen (O_7) or the carbonyl oxygen (O_9) and a quaternary methyl hydrogen, and between the carbonyl oxygen (O_9) and a methylene hydrogen (see Scheme 1 and Figure 1). The gg′ conformation has one three-center hydrogen bond in which a quaternary methyl hydrogen interacts with both the ester oxygen O_7 and the carbonyl oxygen O_9, as well as two other C- -H···O=C hydrogen bonds, more than any other conformer. MP2 results show that the gg′ conformation is the lowest in energy in the gas phase (see Table 2) with gg and gt about 0.8 and 5.7 kJ/mol higher. The tg conformer is 7.5 kJ/mol higher than gg′. This is consistent with previous DFT and MP2 calculations.[2] It also shows the importance of the inclusion of dynamic electron correlation, as in the case of the binding of benzene with $N(CH_3)_4^+$.[62−64]

To more fully evaluate the effect of dynamic electron correlation on the relative energies, gg′ and gg were also optimized at the MP2/6-31G(d) level. Though there are some moderate changes in geometries, especially the shrinkage of the hydrogen bonding distance (up to 0.1 Å), gg′ is still the lowest energy conformation, about 1.4 kJ/mol below the gg form. This demonstrates that energy corrections based on HF optimized geometries are adequate for investigations of this type of structure. It is reasonable to conclude that, in the gas phase, ACh is a mixture of gg′, gg, and gt rotamers. This is also compatible with experimental data[29] for which the ester oxygen atom is gauche to the nitrogen atom.

2. ACh(H_2O)$_m$ ($m = 1$−3). *(a) One Water.* When one water molecule is added, four of the ACh conformations lead to two types of hydrated structures: br, a water bridge is formed between the carbonyl oxygen (electron donor) and the choline moiety; qa, via the water, oxygen (electron donor) binds to a quaternary methyl group (see Figure 2). The backbone structures of most of the hydrated structures are very close to those in the gas phase (Table 1). The exception is the gg′ conformation in which the bridged structure rotates to the gt conformation. Intramolecular hydrogen bonds primarily remain the same as well. Only a few changes are observed in the bridged structures of the gt and tg rotamers. These changes probably occur in order to maximize the formation of intermolecular hydrogen bonds. Assuming that these small changes in dihedral angles and internal hydrogen bonds are due to the effect of solvation, this

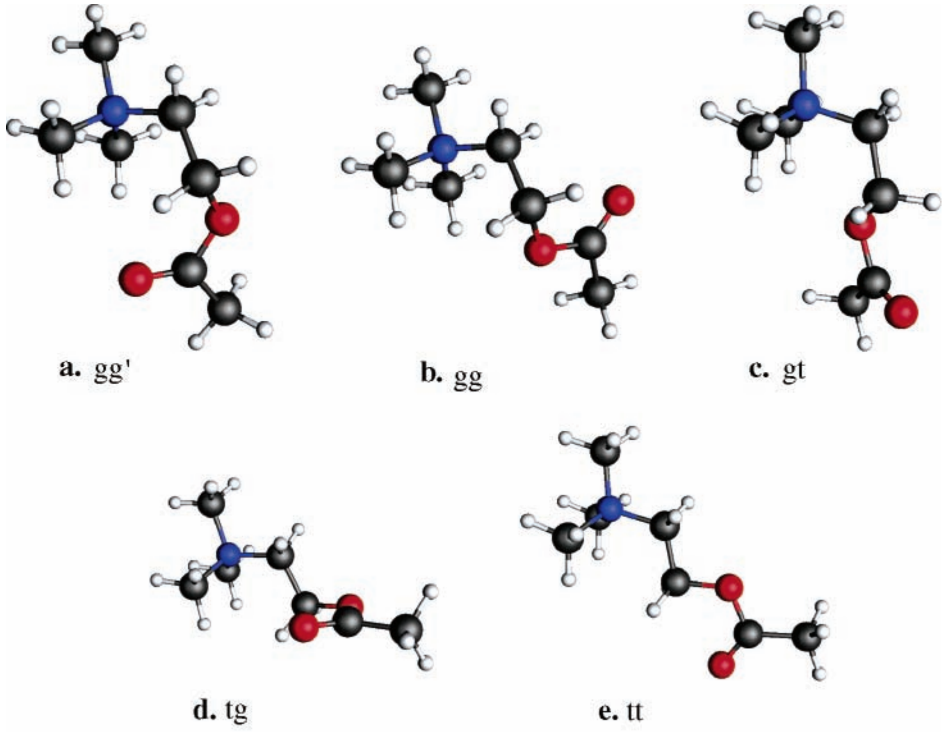
a. gg'
b. gg
c. gt
d. tg
e. tt

Figure 1. Structures of ACh conformers.

implies that adding a water molecule has a limited effect on ACh structures (see Table 3 and Supporting Information).

The gg, gt, and tg bridged structures are listed in Table 3. All of these have intermolecular hydrogen bonds between the carbonyl oxygen and the hydroxyl group of the water molecule (about 2.2 Å at the HF/6-31G(d) level) and between the water oxygen and the quaternary methyl groups (2.4−2.7 Å at the HF/6-31G(d) level, similar to that in the qa structure). Since such a bridge connects the carbonyl oxygen and the choline moiety, it is not surprising that these bridged structures are lower in energy than other hydrated structures, as confirmed in Table 4. Note that the qa structures are less stable by about 7 kJ/mol on average than the corresponding br structures for each rotamer.

In addition to the motivation of understanding the effect of aqueous solvation on ACh and ATCh conformations, it is also of interest to compare the EFP predictions with fully quantum results, both using the 6-31G(d) basis set for the solute. The results in Tables 1 and 3 (and in the Supporting Information) illustrate that the EFP geometries are generally in quite good agreement with the corresponding HF results. The difference in the hydrogen bond length is generally less than 0.1 Å. The most notable exceptions occur for the distances between the carbonyl oxygen and water hydrogen in the bridged structures (EFP1/HF results ∼0.1−0.2 Å longer).

Table 4 lists the relative energies of the ACh$(H2O)_n$ complexes for $n = 1-3$, at several levels of theory, using EFP, HF, and MP2 geometries. For the most part, relative energies based on the geometries optimized at the EFP1/HF/6-31G(d) level are in good agreement with the HF//HF results. For one water, the HF//HF and HF//EFP1 relative energies agree to within 1 kJ/mol. The EFP1//EFP1 results, in which the energy correction is only calculated for the ab initio part (ACh), are reasonably close to both HF//EFP1 and HF//HF relative energies: most deviations are less than 2 kJ/mol. This suggests that the EFP1 method can generate accurate potentials for solvent molecules. Compared with MP2//HF and a few MP2//MP2 results, HF//EFP1 and EFP1//EFP1 can predict semiquantitatively correct relative energies.

It is difficult to identify which rotamer is the lowest in energy among the gg, gt, and tg bridged structures, since they are generally within a few kJ/mol and therefore difficult to rank (distinguish) at these levels of theory. For $n = 1$, the HF/6-31G(d) gg rotamer is the lowest energy structure with gt and tg 2.2 and 0.1 kJ/mol higher. MP2 single point calculations preferentially lower the gg form (the gt and tg forms are 3.6 and 3.7 kJ/mol higher, respectively). MP2/6-31G(d) optimizations enlarge the differences to 3.2 and 4.7 kJ/mol, respectively. MP2/6-311++G(d,p) single point calculations using the MP2/6-31G(d) optimized structures predict that the gg form is 2.4 and 3.1 kJ/mol lower in energy than the gt and tg forms, respectively, so the basis set effects are small. In all cases, these energy differences are within the tolerance of the theoretical methods used. Therefore, one can only conclude that for one water molecule, the bridged structure is energetically preferred, and the br gg, gt, and tg rotamers are lower in energy than other hydrated structures. It is therefore necessary to investigate hydrated structures with additional waters.

(b) Two Waters. When a second water molecule is added (Table 4), there are five possible combinations: (1) qa (first water), qa (second water); (2) qa, w; (3) br, qa; (4) br, w; (5) br, br. As noted above for one water, br structures are generally the lowest in energy. As can be seen in Table 4, this trend carries over to the two water br, br structures. Likewise, the single bridge structures are often lower in energy than those with no bridge. In the two-water bridge structures (C═O···H−O···H−O···H−C) (Figure 2, parts e, g, h, and k), the oxygen atoms from the water molecules can serve as both electron and proton donors, which stabilizes these configurations. Similar structures have been identified as the lowest energy arrangement in the case of diethers and diketones, where the protonated doubly bridged structure can mediate proton transfer between the ether and ketone groups.[65,66] The doubly bridged geometries may be considered to be a common feature in the hydration of polyfunctional ions.[2]

Dihedral angles show similar backbones to their one-water hydrated analogues (see Table 1). In the one water gg′

TABLE 1: Comparisons of Backbone Dihedral Angles (in degrees) of ACh, ACh$(H_2O)_m$ ($m = 1-3$) Calculated at Different Levels of Theory

	$\angle N_1C_5C_6O_7$			$\angle C_5C_6O_7C_8$				$\angle N_1C_5C_6O_7$			$\angle C_5C_6O_7C_8$		
structure	HF[a]	HF[b]	EFP1[c]	HF[a]	HF[b]	EFP1[c]	structure	HF[a]	HF[b]	EFP1[c]	HF[a]	HF[b]	EFP1[c]
ACh													
gg′	77.8	78.1		−112.8	−112.6		tg	−161.0	−155.6		80.4	79.8	
gg	67.3	67.3		78.7	78.7		tt	180.0	180.0		180.0	180.0	
gt	62.6	62.5		171.3	171.1								
ACh(H_2O)													
gg′, qa	78.0	78.4	78.5	−113.5	−113.8	−113.6	tg, br	175.3	−169.7	175.4	83.4	86.9	83.8
gg, br	67.3	72.6	67.4	76.5	85.0	76.8	tg, qa	−164.6	−161.2	−164.1	81.1	80.7	81.1
gg, qa	68.3	68.3	68.2	79.2	78.9	78.9	tt, br	180.0	180.0	180.0	180.0	180.0	180.0
gt, br	83.2	83.2	82.8	−167.2	−167.2	−165.2	tt, qa	180.0	180.0	180.0	180.0	180.0	180.0
gt, qa	62.4	63.9	62.5	172.2	171.6	172.6							
ACh$(H_2O)_2$													
gg′, qa, qa	78.5	78.4	78.2	−114.7	−114.4	−114.2	gt, br, br	77.4	76.6	79.2	178.2	179.4	176.3
gg′, qa, w	79.0	78.9	78.0	−115.3	−114.9	−114.4	tg, qa, qa	−164.3	−165.0	−165.3	81.8	81.7	81.4
gg′, br, br	88.0	N/A	87.5	−141.0	N/A	−137.7	tg, qa, w	−165.8	−169.2	−165.6	81.7	81.8	81.7
gg, qa, qa	68.8	74.5	69.8	79.4	77.1	79.2	tg, br, qa	−171.2	−171.5	−170.5	87.0	87.2	86.5
gg, qa, w	69.0	69.4	69.3	78.5	79.0	78.7	tg, br, w	175.5	−162.2	175.4	84.2	86.0	84.3
gg, br, qa	73.4	73.5	73.7	85.0	84.8	84.0	tg, br, br	−167.6	N/A	−167.4	88.7	N/A	89.1
gg, br, w	69.9	71.8	68.3	77.3	84.1	78.1	tt, qa, qa	−178.5	179.0	180.0	180.0	−179.6	180.0
gg, br, br	72.2	N/A	72.1	85.5	N/A	84.8	tt, qa, w	180.0	179.9	180.0	180.0	179.7	180.0
gt, qa, qa	65.5	63.7	64.1	171.5	172.8	172.5	tt, br, qa	179.1	180.0	180.0	180.0	180.0	180.0
gt, qa, w	63.4	64.9	63.2	172.1	171.9	172.9	tt, br, w	180.0	180.0	180.0	180.0	180.0	180.0
gt, br, qa	83.5	64.9	82.7	−168.5	171.9	−170.0	tt, br, br	175.4	N/A	180.0	176.7	N/A	180.0
gt, br, w	81.3	81.2	81.2	−170.4	−169.8	−167.7							
ACh$(H_2O)_3$													
gg′, qa, qa, w			77.7			−114.5	gt, br, br, w			78.3			177.6
gg′, qa, qa, qa			77.9			−114.6	gt, br, br, br			78.0			180.0
gg′, br, br, qa			86.8			−138.1	tg, qa, w, br			−172.2			86.7
gg′, br, br, br			86.2			−135.2	tg, qa, qa, w			−163.8			81.9
gg, qa, w, br			73.8			84.0	tg, qa, qa, br			−171.1			86.8
gg, qa, qa, br			68.1			77.0	tg, qa, qa, qa			−168.2			82.5
							tg, br, w, qa			−168.9			82.8
							tg, br, br, qa			−167.6			90.1
gg, br, w, qa			73.0			83.7	tg, br, br, w			−169.0			89.5
gg, br, br, qa			72.2			85.2	tg, br, br, br			176.4			87.6
gg, br, br, w			72.0			86.9	tt, qa, w, br			177.8			180.0
gg, br, br, br			77.8			79.8	tt, qa, qa, w			−177.5			−179.2
gt, qa, w, br			83.1			−167.5	tt, qa, qa, br			180.0			180.0
gt, qa, qa, w			64.3			170.4	tt, qa, qa, qa			−179.2			180.0
gt, qa, qa, br			82.9			−166.3	tt, br, w, qa			180.0			180.0
gt, qa, qa, qa			65.3			173.1	tt, br, br, qa			176.2			177.6
gt, br, w, qa			81.8			−168.8	tt, br, br, w			176.2			177.1
gt, br, br, qa			79.3			176.7	tt, br, br, br			175.9			177.2

[a] HF/6-31G(d) results. [b] Values are taken from ref 2. [c] EFP1/HF/6-31G(d) results.

TABLE 2: HF/6-31G(d) Hydrogen Bond Lengths, Angles, and Relative Energies for the Gas Phase ACh Rotamers[a]

	$O_7\cdots H$	angle[b]	$O_9\cdots H$	angle[b]	ΔE_{HF} [c]	ΔE_{MP2}[d]	ΔE_{MP2} [e]
gg′	2.722 (13)	108.3	2.405 (13)	147.8	0.0	0.0	0.0
			2.495 (15)	145.3			
			2.319 (23)	97.5			
gg	2.398 (13)	116.9	2.524 (20)	109.9	−0.2	1.8	1.4
gt	2.309 (13)	122.0	2.511 (23)	81.8	2.1	5.7	
tg			2.503 (21)	108.5	1.7	7.5	
tt					8.0	18.0	

[a] Hydrogen bonding distances in angstroms, angles in degrees, and relative energies in kilojoules per mole. See Scheme 1 for atom numbering system. Numbers in parentheses indicate hydrogen to which the oxygen is hydrogen bonded. [b] Angle O•••H−C. [c] HF/6-31G(d)//HF/6-31G(d). [d] MP2/6-31G(d)//HF/6-31G(d). [e] MP2/6-31G(d)//MP2/6-31G(d).

conformation, the distance between the carbonyl oxygen and the closest methyl group is too short to form a stable one-water bridge, instead of a direct hydrogen bond. A two-water system makes it possible to reach a distant methyl group. However, the introduction of the two-water bridge pushes the carbonyl away. This rearrangement is reflected in the gg′, br, br backbone dihedral angle, $\angle C_5C_6O_7C_8 \sim -137°$. This angle is much larger than that in gas phase gg′, as the structure is rotated toward the gt conformation.

Hydrogen bond lengths of the lowest energy structures are listed in Table 5. A more extensive list of structures is provided in the Supporting Information. The relative energies can be found in Table 4. Adding the second water molecule does not significantly change the hydrogen bond distances involving the first water molecule. The conformations containing a two-water bridge have relatively shorter distances (independent of the conformation type) between the carbonyl oxygen and the hydrogen atom of the first water, between the first oxygen and the hydroxyl group of the second water, and between the second oxygen and the quaternary methyl group (about 2.1, 1.9, and 2.4 Å, respectively). The relative energies (Table 4) reveal that the doubly bridged structure is the lowest energy arrangement for each conformation. The lowest energy conformer is gg, br, br, with gt, br, br about 2.5, 3.2, and 4.9 kJ/mol higher at the HF//HF, MP2//HF, and MP2//MP2 levels, respectively. The remaining isomers tt, br, br and tg, br, br are 3.9 and 7.9 kJ/mol higher than gg, br, br, respectively, at the HF level. MP2

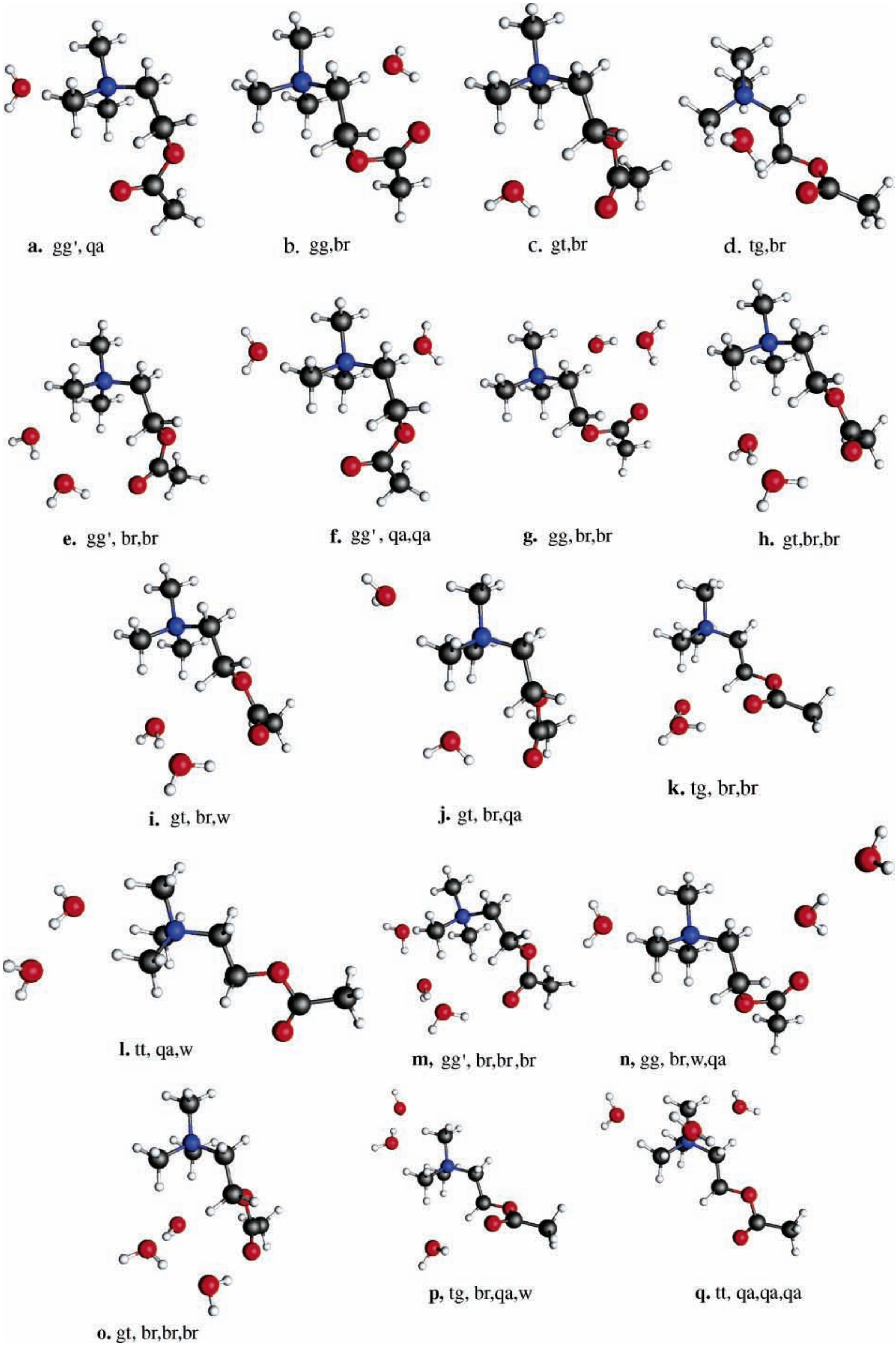

a. gg', qa

b. gg,br

c. gt,br

d. tg,br

e. gg', br,br

f. gg', qa,qa

g. gg, br,br

h. gt,br,br

i. gt, br,w

j. gt, br,qa

k. tg, br,br

l. tt, qa,w

m, gg', br,br,br

n, gg, br,w,qa

o. gt, br,br,br

p, tg, br,qa,w

q. tt, qa,qa,qa

Figure 2. Structures of some ACh(H_2O)$_m$ ($m = 1-3$) structures.

TABLE 3: HF/6-31G(d) and EFP1/HF/6-31G(d) Hydrogen Bond Lengths and Angles for Several ACh(H_2O) Structures[a,b]

		$O_7 \cdots H$	angle[c]	$O_9 \cdots H$	angle[c]	$O_{27} \cdots H$	angle[c]
gg, br	EFP1	2.412 (13)	113.8	2.530 (20)	110.2	2.419 (11)	151.2
				2.484 (22)	86.8	2.704 (19)	141.7
				2.442 (28)	127.2	2.447 (20)	150.3
	HF	2.419 (13)	113.6	2.531 (20)	110.4	2.453 (11)	148.8
				2.488 (22)	86.7	2.700 (19)	141.0
				2.243 (28)	134.2	2.343 (20)	152.7
gt,br	EFP1	2.634 (13)	98.8	2.385 (23)	91.4	2.467 (13)	151.7
				2.318 (28)	134.1	2.411 (15)	151.1
						2.605 (23)	138.5
	HF	2.639 (13)	98.5	2.408 (23)	90.3	2.519 (13)	152.0
				2.175 (28)	138.9	2.408 (15)	154.1
						2.444 (23)	141.6
tg,br	EFP1			2.592 (21)	109.1	2.289 (15)	153.0
				2.415 (23)	90.2	2.744 (18)	138.2
				2.238 (28)	140.5	2.472 (21)	140.2
	HF			2.600 (21)	108.9	2.320 (15)	150.3
				2.412 (23)	90.2	2.698 (18)	138.2
				2.113 (28)	146.3	2.370 (21)	142.4

[a] Hydrogen bonding distances in angstroms and angles in degrees. See Scheme 1 for atom numbering system. Numbers in parentheses indicate hydrogen to which oxygen is hydrogen bonded. [b] Numbering scheme for water molecules: $H_{28}O_{27}H_{29}$. [c] Angle $O \cdots H-X$, where $X = C$ or O.

energy corrections increase these relative energies to 9.6 and 12.0 kJ/mol (HF geometries), and 7.8 and 11.7 kJ/mol (MP2 geometries), respectively.

Comparisons between the HF and EFP1/HF results reveal that, though there are some deviations, the HF//EFP1 and EFP1//EFP1 results are generally in good agreement with the much more time-consuming fully ab initio results. The EFP1 and HF relative energies generally agree to within 2−4 kJ/mol, and the important trends are preserved. In particular, the two methods agree that the br, br conformers are among the lowest in energy. Therefore, geometry optimizations for three waters are done only with the EFP1/HF method.

(c) Three Waters. With three waters, one can have one-, two-, or even three-water bridges. Eight combinations are found: (1) qa (first water), w (second water), br (third water); (2) qa, qa, w; (3) qa, qa, br; (4) qa, qa, qa; (5) br, w, qa; (6) br, br, qa; (7) br, br, w; (8) br, br, br (see Figure 2). Dihedral angles are listed in Table 1 and hydrogen bond parameters are given in Supporting Information. The dihedral angles are generally close to those of the gas-phase ACh rotamers, except for a few changes in gt and tg bridged structures. The gg′, br, br, br and gg′, br, br, qa dihedral angles $N_1C_5C_6O_7$ and $C_5C_6O_7C_8$ again rotate so that the water bridge occurs between the carbonyl oxygen and distant methyl groups. A consequence of this rotation is that the complex becomes close in structure to that of the gt conformer.

As for ACh(H_2O)$_2$, the hydrated structures containing a three-water bridge are always lower in energy than other isomers with the same conformation. gg, br, br, br is the most stable structure; gt, br, br, br is 1.8 kJ/mol higher at the HF level, with gg′, br, br, br; tt, br, br, br; and tg, br, br, br 2.7, 2.4, and 5.4 kJ/mol higher, respectively. The corresponding EFP1/HF relative energies are 3.4, 6.7, 4.1, and 7.4 kJ/mol, respectively. This suggests that for three waters, the lowest energy structures are likely to be either of the gg or gt type in solution. However, all of these br, br, br species are within a small energy range.

Although no one conformation can be described as being predominant in aqueous solution, the computational results suggest that hydration may stabilize more than one conformation (in this case gg and gt, since these rotamers have more low energy forms than the other three). This suggestion is consistent with ^{1}H and ^{13}C NMR,[17−18] as well as Raman experiments,[19] which indicate that both gg and gt conformations coexist in aqueous solution. The gt form is preferred; however, the gg form also displays significant population (31.2% at 10 °C and 37.5% at 70 °C).[18]

3. ATCh. Five conformations, gg′, gg, gt, tg, and tt, similar to ACh, are found for ATCh (see Figure 3). Table 6 lists the dihedral angles $N_1C_5C_6S_7$ and $C_5C_6S_7C_8$. The values for $C_4N_1C_5C_6$ and $C_6S_7C_8C_{10}$ are close to 180° and are omitted from the table. ATCh has very similar backbone structures to ACh. Taking into account that the sulfur atom has a bigger van der Waals radius than the oxygen atom (1.02 vs 0.73 Å), the five rotamers of ATCh demonstrate the same kinds of intramolecular hydrogen bonds as those of ACh (see Table 7). Consider the distance between the carbonyl oxygen and the nitrogen for ATCh relative to ACh. The $C_6-S_7-C_8$ angle ranges from 98 to 101°. This range is much smaller than that of 116−119° for the analogous angle in ACh, because bonds to S have primarily *p* character, whereas O exhibits more s−p mixing. Compare, for example, H_2O with an HOH bond angle of ∼104° vs H_2S with an HSH bond angle of ∼92°. Although the sulfur atom is pushed away from the choline moiety relative to oxygen, the smaller $C_6-S_7-C_8$ angle pulls the carbonyl oxygen atom back. The O_9-N_1 distance is therefore similar in the O and S species. This suggests that ATCh and ACh may have similar types of intermolecular hydrogen bonds and, hence, similar hydrated structures.

Although ATCh has similar structures to ACh, differences are observed in the relative energies (see Table 7). Unlike ACh with several rotamers close in energy, in gas phase ATCh there are just two low energy rotamers at the MP2 level of theory, namely the global minimum tg and gg′, 4.9 kJ/mol less stable.

4. ATCh(H_2O)$_n$ ($n = 1$−3). *(a) One Water.* With one water molecule present, both br and qa structures are found for ATCh rotamers (see Figure 4). Table 6 gives dihedral angles for the one-water hydrated structures. The backbone structures of ATCh(H_2O) generally remain the same as their gas-phase structures. Like ACh(H_2O), only a few changes are observed in gt and tg bridged structures, due to the solvent.

The relative energies (see Table 8) show that, as found for ACh(H_2O), the bridged structures of ATCh(H_2O) are the lowest in energy by 4−6 kJ/mol. An exception is the gg′ rotamer, for which br is 6 kJ/mol higher in energy than qa. The relative

TABLE 4: Relative Energies (in kJ/mol) for ACh$(H_2O)_m$ (m = 1−3) at Different Levels of Theory Using the 6-31G(d) Basis Set

species	ΔE_{HF}[a]	ΔE_{HF}[b]	ΔE_{MP2}[c]	ΔE_{EF}[d]	ΔE_{MP2}[e]
ACh(H_2O), gg′, qa	7.5	6.9	5.4	6.3	
ACh(H_2O), gg, br	−0.1	−0.1	−3.7	0.0	−4.7
ACh(H_2O), gg, qa	6.6	6.2	6.6	5.8	
ACh(H_2O), gt, br	2.1	2.2	−0.1	2.8	−1.5
ACh(H_2O), gt, qa	8.9	8.4	10.0	8.0	
ACh(H_2O), tg, br	0.0	0.0	0.0	0.8	0.0
ACh(H_2O), tg, qa	8.2	7.9	12.0	7.5	
ACh(H_2O), tt, br	7.9	8.4	10.5	9.1	
ACh(H_2O), tt, qa	13.7	12.9	20.3	13.1	
ACh$(H_2O)_2$, gg′, qa, qa	15.0	12.8	18.3	13.6	
ACh$(H_2O)_2$, gg′, qa, w	12.7	10.6	15.5	14.1	
ACh$(H_2O)_2$, gg′, br, br	9.8	8.6	10.4	11.0	
ACh$(H_2O)_2$, gg, qa, qa	12.3	10.4	18.3	12.3	
ACh$(H_2O)_2$, gg, qa, w	10.9	8.5	15.3	12.4	
ACh$(H_2O)_2$, gg, br, qa	13.4	7.7	19.4	15.1	19.9
ACh$(H_2O)_2$, gg, br, br	0.0	0.7	0.0	0.0	−4.9
ACh$(H_2O)_2$, gg, br, w	6.1	8.2	8.5	8.8	
ACh$(H_2O)_2$, gt, qa, qa	15.8	13.7	22.9	14.9	
ACh$(H_2O)_2$, gt, qa, w	13.3	11.0	18.9	14.8	
ACh$(H_2O)_2$, gt, br, qa	8.1	4.9	11.9	8.9	10.3
ACh$(H_2O)_2$, gt, br, br	2.5	0.0	3.2	3.6	0.0
ACh$(H_2O)_2$, gt, br, w	9.1	7.8	12.8	12.1	12.9
ACh$(H_2O)_2$, tg, qa, qa	14.6	12.1	24.1	14.6	
ACh$(H_2O)_2$, tg, qa, w	12.2	9.7	20.0	13.5	
ACh$(H_2O)_2$, tg, br, qa	14.0	10.9	21.1	14.4	20.1
ACh$(H_2O)_2$, tg, br, br	7.9	5.4	12.0	7.9	11.7
ACh$(H_2O)_2$, tg, br, w	7.6	6.3	13.4	11.3	14.5
ACh$(H_2O)_2$, tt, qa, qa	19.2	16.6	31.5	19.1	
ACh$(H_2O)_2$, tt, qa, w	17.0	14.4	27.7	18.4	
ACh$(H_2O)_2$, tt, br, qa	12.8	9.4	21.3	13.0	
ACh$(H_2O)_2$, tt, br, br	3.9	0.9	9.6	5.4	7.8
ACh$(H_2O)_2$, tt, br, w	14.4	12.8	23.7	17.0	
ACh$(H_2O)_3$, gg′, qa, qa, w		12.0		14.7	
ACh$(H_2O)_3$, gg′, qa, qa, qa		16.7		14.3	
ACh$(H_2O)_3$, gg′, br, br, qa		10.3		9.8	
ACh$(H_2O)_3$, gg′, br, br, br		2.7		3.3	
ACh$(H_2O)_3$, gg, qa, w, br		11.4		12.9	
ACh$(H_2O)_3$, gg, qa, qa, br		7.3		6.3	
ACh$(H_2O)_3$, gg, br, w, qa		20.4		21.5	
ACh$(H_2O)_3$, gg, br, br, qa		1.0		0.5	
ACh$(H_2O)_3$, gg, br, br, w		4.2		4.7	
ACh$(H_2O)_3$, gg, br, br, br		−1.8		−3.4	
ACh$(H_2O)_3$, gt, qa, w, br		7.0		8.8	
ACh$(H_2O)_3$, gt, qa, qa, w		15.6		14.4	
ACh$(H_2O)_3$, gt, qa, qa, br		10.5		9.9	
ACh$(H_2O)_3$, gt, qa, qa, qa		17.5		14.1	
ACh$(H_2O)_3$, gt, br, w, qa		11.4		13.0	
ACh$(H_2O)_3$, gt, br, br, qa		3.4		4.0	
ACh$(H_2O)_3$, gt, br, br, w		6.9		9.4	
ACh$(H_2O)_3$, gt, br, br, br		0.0		0.0	
ACh$(H_2O)_3$, tg, qa, w, br		12.7		15.2	
ACh$(H_2O)_3$, tg, qa, qa, w		14.2		13.6	
ACh$(H_2O)_3$, tg, qa, qa, br		14.9		14.0	
ACh$(H_2O)_3$, tg, qa, qa, qa		18.8		15.5	
ACh$(H_2O)_3$, tg, br, w, qa		9.8		11.6	
ACh$(H_2O)_3$, tg, br, br, qa		8.3		8.0	
ACh$(H_2O)_3$, tg, br, br, w		11.8		12.3	
ACh$(H_2O)_3$, tg, br, br, br		3.6		4.0	
ACh$(H_2O)_3$, tt, qa, w, br		12.1		11.8	
ACh$(H_2O)_3$, tt, qa, qa, w		18.5		17.7	
ACh$(H_2O)_3$, tt, qa, qa, br		13.2		14.2	
ACh$(H_2O)_3$, tt, qa, qa, qa		21.3		19.5	
ACh$(H_2O)_3$, tt, br, w, qa		15.4		17.2	
ACh$(H_2O)_3$, tt, br, br, qa		4.0		4.0	
ACh$(H_2O)_3$, tt, br, br, w		9.1		12.8	
ACh$(H_2O)_3$, tt, br, br, br		0.6		0.7	

[a] HF/6-31G(d)//HF/6-31G(d). [b] HF/6-31G(d)//EFP1/HF/6-31G(d). [c] MP2/6-31G(d)//HF/6-31G(d). [d] EFP1/HF/6-31G(d)//EFP1/-HF/6-31G(d). [e] MP2/6-31G(d)//MP2/6-31G(d).

energies are more spread out for ATCh(H_2O): tg, br is the lowest energy structure, and tg, qa is 5.8 (7.5) kJ/mol higher using HF//HF (MP2//HF). Other conformations are at least 14−15 kJ/mol higher.

Table 9 gives the gg, gt, and tg bridged structures. The hydrogen bond distances and associated angles predicted by the EFP method are in good agreement with the HF values, with differences in bond distances generally <0.1 Å. The relative energies (Table 8) based on EFP1 optimized geometries are very close to those using HF geometries. For one water, HF//HF and HF//EFP1 relative energies agree to within 0.5 kJ/mol. EFP1//EFP1 relative energies, though not as good as HF//EFP1, still agree with HF//HF to within 2 kJ/mol. Again, both EFP1//EFP1 and HF//EFP1 results are comparable with MP2//HF.

(b) Two Waters. When two water molecules are present, similar arrangements to ACh are found: qa, qa; qa, w; br, qa; br, w; and br, br (see Figure 4). The backbone structures are similar to ATCh in the gas phase (see Table 6) with some changes observed relative to ATCh(H_2O) for the gt and tg bridged structures.

The hydrogen bond distances and associated angles for the tg conformation are listed in Table 10. The complete results of ATCh$(H_2O)_2$ can be found in the Supporting Information. HF and EFP1/HF predict very similar geometries. The hydrogen bond distances and associated angles predicted by the EFP1 method agree well with the HF results, with differences in bond distances generally <0.1 Å (with a few exceptions up to 0.2 Å) for ATCh(H_2O) and ATCh$(H_2O)_2$.

The relative energies are listed in Table 8. The lowest energy structures all correspond to the tg conformation. Although the lowest energy structure has a double bridge, the remaining low energy species are not dominated by water bridges as they are in ACh$(H_2O)_n$. ATCh$(H_2O)_2$, tg, br, w lies 2.9 and 6.7 kJ/mol above ATCh$(H_2O)_2$, tg, br, br according to HF//HF and MP2//HF, respectively. The other three conformations are at least 5 (11) kJ/mol higher in energy at the HF (MP2) level. These results are in good agreement with the observation discussed above that bridged structures are preferred in the solvation of ATCh(H_2O), but the relative energies are mainly determined by the gas-phase structures. The HF//EFP1 and HF//HF relative energies agree to within 2 kJ/mol. The EFP1//EFP1 relative energies predict the correct trends and are within 4 kJ/mol of the more time-consuming HF//HF results.

(c) Three Waters. On the basis of the success of the EFP method, the geometries of ATCh$(H_2O)_3$ are optimized only at the EFP1/HF level. Conformations similar to ACh are found, including those with one-, two- or three-water bridges. Dihedral angles (see Table 6) show that ATCh$(H_2O)_3$ exhibits the same trends as were observed in ATCh(H_2O) and ATCh$(H_2O)_2$: they are quite close to the gas phase structures with only a few exceptions due to solvent effects.

The relative energies of ATCh$(H_2O)_3$ are listed in Table 8. The tg conformations are consistently predicted to be lower in energy than any other rotamer. The highest energy tg conformation (qa, qa, qa) has the same relative energy as the lowest energy non-tg rotamer (gg, br, br, qa). This is in good agreement with ATCh(H_2O) and ATCh$(H_2O)_2$. The three-water bridge is not always the lowest energy structure. The HF//EFP1 (EFP1//EFP1) results demonstrate that tg, br, br, qa is the most stable structure and tg, br, br, w and tg, br, br, br are 2.2(0.6) and 3.6(2.2) kJ/mol higher, respectively. The other conformations are at least 4 kJ/mol higher. The ATCh results presented here for up to three water molecules suggest that the tg form should

TABLE 5: HF/6-31G(d) and EFP1/HF/6-31G(d) Hydrogen Bond Lengths and Angles for Several ACh(H_2O)$_2$ Structures[a,b]

		$O_7\cdots H$	angle [c]	$O_9\cdots H$	angle [c]	$O_{27}\cdots H$	angle[c]	$O_{30}\cdots H$	angle[c]
gg, br,br	EFP1	2.433 (13)	113.3	2.746 (20)	105.6	2.670 (20)	153.0	2.354 (11)	148.6
				2.379 (22)	92.2	1.958 (31)	156.0	2.340 (19)	149.3
				2.186 (28)	140.4			2.647 (20)	141.5
	HF	2.435 (13)	112.5	2.777 (20)	105.2	2.738 (20)	150.1	2.372 (11)	148.2
				2.375 (22)	92.6	1.904 (31)	160.4	2.386 (19)	147.7
				2.076 (28)	143.8			2.512 (20)	144.9
gt, br,qa	EFP1	2.610 (13)	100.5	2.402 (23)	90.3	2.523 (13)	151.7	2.921 (12)	139.7
				2.330 (28)	133.5	2.441 (15)	153.0	2.479 (16)	153.4
						2.624 (23)	136.5	2.422 (18)	154.5
	HF	2.641 (13)	99.0	2.173 (28)	139.1	2.574 (13)	152.5	2.813 (12)	142.8
						2.465 (15)	154.9	2.511 (16)	152.5
						2.435 (23)	142.4	2.466 (18)	154.3
gt, br,br	EFP1	2.532 (13)	102.8	2.183 (28)	140.7	2.712 (23)	146.1	2.428 (13)	147.0
						1.947 (31)	159.1	2.311 (15)	151.9
								2.772 (23)	130.6
	HF	2.503 (13)	103.5	2.077 (28)	142.9	2.674 (23)	144.5	2.431 (13)	150.4
						1.894 (31)	162.4	2.343 (15)	154.3
								2.639 (23)	127.6
tg, br,br	EFP1			2.750 (21)	105.3	2.459 (15)	149.4	2.354 (13)	158.0
				2.380 (23)	81.9	2.034 (31)	148.6	2.612 (15)	141.2
				2.177 (28)	147.1			2.455 (23)	139.9
	HF			2.600 (21)	108.9	2.320 (15)	146.8	2.320 (13)	150.3
				2.412 (23)	90.2	1.960 (31)	150.3	2.698 (15)	138.2
				2.113 (28)	146.3			2.440 (23)	142.4
tt, br,br	EFP1			2.058 (28)	139.0	1.910 (31)	163.0	2.302 (13)	153.0
								2.298 (15)	138.2
	HF			2.011 (28)	155.9	2.761 (23)	127.7	2.285 (13)	151.0
						1.870 (21)	165.1	2.337 (15)	151.4
								2.707 (22)	116.3

[a] Hydrogen bonding distances in angstroms and angles in degrees. See Scheme 1 for atom numbering system. Numbers in parentheses indicate the hydrogen to which oxygen is hydrogen bonded. [b] Numbering scheme for water molecules: $H_{28}O_{27}H_{29}$ and $H_{31}O_{30}H_{32}$. [c] Angle O$\cdots$H$-$X, where X = C or O.

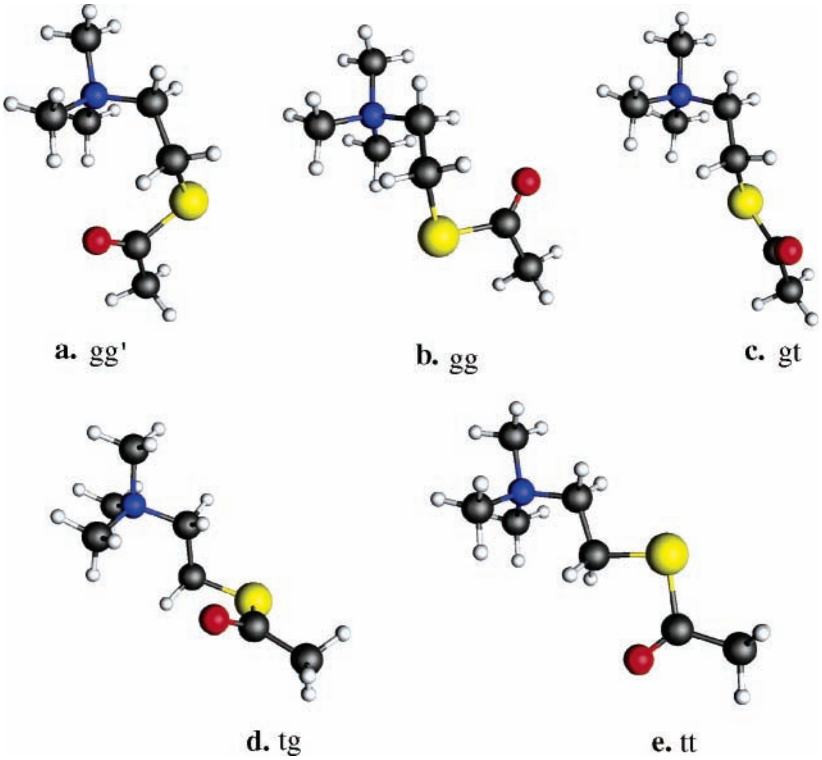

Figure 3. Structures of ATCh conformers.

be predominant in aqueous solution. This result is consistent with the experimental data.[67]

5. Comparison of ACh and ATCh

Apparently, solvation has only small effects on the geometries of both ACh and ATCh. Hydrated structures are generally similar to the gas phase structures and the water bridge is the favored arrangement for binding water molecules. The relative stabilities of the hydrated structures are mainly determined by the gas-phase structures. The gg′, gg, and gt ACh conformers are lowest in energy in the gas phase, while gg and gt conformers are lowest in energy in the presence of one to three

TABLE 6: Comparisons of Backbone Dihedral Angles (in degrees) of ATCh, ATCh(H_2O)$_n$ (n = 1−3) Calculated at Different Levels of Theory

	$\angle N_1C_5C_6S_7$		$\angle C_5C_6S_7C_8$			$\angle N_1C_5C_6S_7$		$\angle C_5C_6S_7C_8$	
structure	HF[a]	EFP1[b]	HF[a]	EFP1[b]	structure	HF[a]	EFP1[b]	HF[a]	EFP1[b]
					ATCh				
gg′	82.9		−108.3		tg	−167.4		77.1	
gg	71.6		70.5		tt	180.0		180.0	
gt	77.3		157.2						
					ATCh(H_2O)				
gg′, br	86.0	86.0	−112.1	−112.4	gt, qa	87.4	88.2	168.6	169.0
gg′, qa	83.7	83.6	−109.0	−109.1	tg, br	177.6	177.7	79.1	79.1
gg, br	70.5	70.5	67.3	67.6	tg, qa	−169.0	−168.9	77.1	77.2
gg, qa	72.5	72.6	72.3	72.1	tt, br	180.0	180.0	180.0	180.0
gt, br	98.0	98.1	−122.0	−121.9	tt, qa	180.0	180.0	180.0	180.0
					ATCh(H_2O)$_2$				
gg′, qa,qa	84.2	84.0	−110.2	−109.5	gt, br,w	96.3	97.6	−119.9	−119.9
gg′, qa,w	83.7	83.3	−109.9	−109.5	gt, br,br	96.1	94.1	174.2	174.8
gg′, br,qa	88.6	87.8	−115.7	−114.7	tg, qa,qa	−170.2	−171.3	78.0	77.8
gg′, br,w	85.3	86.1	−110.3	−113.5	tg, qa,w	−170.6	−171.5	77.4	77.8
gg′, br,br	87.3	87.8	−111.4	−112.1	tg, br,qa	−172.2	−172.8	80.3	80.2
gg, qa,qa	91.2	90.1	73.2	72.8	tg, br.w	177.3	177.4	79.7	79.6
gg, qa,w	89.9	89.7	73.6	73.8	tg, br.br	−176.2	−177.0	83.9	84.2
gg, br,qa	91.9	91.0	76.1	75.9	tt, qa,qa	180.0	180.0	180.0	180.0
gg, br,w	73.5	71.6	68.5	68.8	tt, qa,w	180.0	180.0	180.0	180.0
gg, br,br	84.5	84.6	74.1	74.5	tt, br,qa	180.0	180.0	180.0	180.0
gt, qa,qa	86.2	85.4	164.0	164.9	tt, br,w	180.0	180.0	180.0	180.0
gt, qa,w	86.3	88.2	165.7	172.6					
					ATCh(H_2O)$_3$				
gg′, qa,w,br		88.7		−115.6	gt, qa,qa,qa		85.8		164.3
gg′, qa,qa,w		83.8		−109.9	gt, br,br,qa		94.6		174.6
gg′, qa,qa,br		88.0		−114.3	gt, br,br,w		94.4		175.5
gg′, qa,qa,qa		83.8		−109.9	gt, br,br,br		94.7		174.5
gg′, br,w,qa		87.6		−116.3	tg, qa,w,br		−173.0		78.9
gg′, br,br,qa		87.3		−113.4	tg, qa,qa,w		−168.5		78.4
gg′, br,br,w		87.0		−112.1	tg, qa,qa,br		−173.8		79.8
gg′, br,br,br		89.5		−116.0	tg, qa,qa,qa		−171.4		78.0
gg, qa,w,br		91.9		76.8	tg, br,w,qa		177.0		80.2
gg, qa,qa,w		90.7		73.6	tg, br,br,qa		−176.8		84.3
gg, qa,qa,br		91.0		74.0	tg, br,br,w		−174.1		83.4
gg, qa,qa,qa		91.1		73.7	tg, br,br,br		−178.1		79.9
gg, br,w,qa		91.1		75.7	tt, qa,w,br		180.0		180.0
gg, br,br,qa		84.7		74.6	tt, qa,qa,w		180.0		−176.8
gg, br,br,w		84.3		75.2	tt, qa,qa,br		180.0		180.0
gg, br,br,br		94.5		78.6	tt, qa,qa,qa		180.0		180.0
gt, qa,qa,w		85.6		164.7	tt, br,w,qa		180.0		180.0

[a] HF/6-31G(d) results. [b] EFP1/HF/6-31G(d) results.

TABLE 7: HF/6-31G(d) Hydrogen Bond Lengths, Angles, and Relative Energies for the Gas Phase ATCh Rotamers[a]

	$S_7 \cdots H$	angle[b]	$O_9 \cdots H$	angle[b]	ΔE_{HF}[c]	ΔE_{MP2}[d]
gg′	2.957 (13)	113.6	2.414 (13)	151.2	10.8	4.9
			2.474 (15)	148.7		
			2.389 (23)	106.7		
gg	2.757 (13)	134.3	2.460 (20)	116.6	15.6	13.6
gt	2.715 (13)	116.1	2.389 (23)	100.5	23.6	22.5
tg			2.494 (21)	113.6	0.0	0.0
tt					16.6	20.3

[a] Hydrogen bonding distances in angstroms, angles in degrees, and relative energies in kilojoules per mole. See Scheme 1 for atom numbering system. Numbers in parentheses indicate the hydrogen to which oxygen or sulfur is hydrogen bonded. [b] Angle Y···H−C where Y = S or O. [c] HF/6-31G(d)//HF/6-31G(d). [d] MP2/6-31G(d)//HF/6-31G(d).

waters. The tg ATCh conformer is always lowest in energy in both gas phase and in the presence of waters. It is interesting that ACh always prefers the gauche form of $N_1C_5C_6O_7$, whereas ATCh prefers trans $N_1C_5C_6S_7$.

Population analyses suggest that the positive charge is spread onto the exterior surfaces of the methyl and methylene groups bound to the nitrogen, with negative charges on the N, ester oxygen, and carbonyl oxygen in ACh (see Table 11) that are similar to previous studies.[48] Therefore, instead of a positive charge on N itself, a “cationic head” is formed. It is therefore possible that electrostatic interactions between the terminal hydrogens in the methyl groups and the ester oxygen may lead to a heterocyclic six-member ring. For the purpose of comparison, if ACh is replaced by 2,2-dimethylbutyl ester, a neutral and isoelectronic analogue of the choline ester, none of its numerous conformations exhibit the close intramolecular contact between the ester oxygen and a terminal methyl observed in ACh.[23] This result lends support to the notion that the positive charge associated with the quaternary nitrogen group in choline stabilizes the gauche form of the ester oxygen relative to the nitrogen and embraces the close interactions between the ester oxygen and the methyl groups attached to the nitrogen. Therefore, strong electrostatic interactions, in addition to relatively weaker intramolecular hydrogen bonds, are expected between the ester oxygen and the positive exterior of the cationic head in the case of the gg′, gg, and gt conformations. These interactions enhance the stabilities of these rotamers in the gas phase. In ATCh, although the “cationic head” is similar, the sulfur atom is not as electronegative as the oxygen (see Table

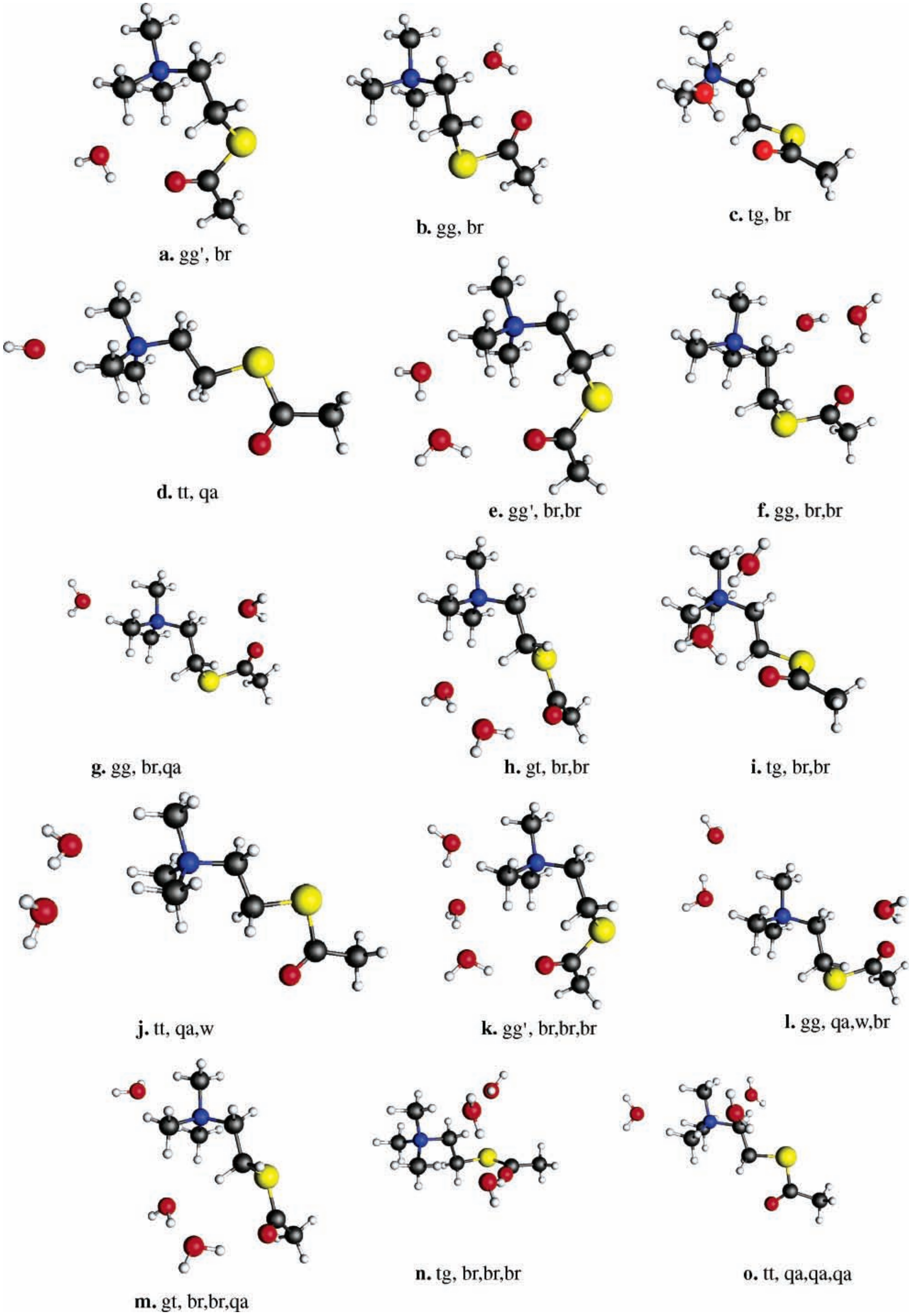

a. gg′, br

b. gg, br

c. tg, br

d. tt, qa

e. gg′, br,br

f. gg, br,br

g. gg, br,qa

h. gt, br,br

i. tg, br,br

j. tt, qa,w

k. gg′, br,br,br

l. gg, qa,w,br

m. gt, br,br,qa

n. tg, br,br,br

o. tt, qa,qa,qa

Figure 4. Structures of some ATCh(H_2O)$_n$ (n = 1−3) complexes.

TABLE 8: Relative Energies (in kJ/mol) for ATCh$(H_2O)_n$ ($n = 1-3$) at Different Levels of Theory Using the 6-31G(d) Basis Set

species	ΔE_{HF} [a]	ΔE_{HF} [b]	ΔE_{MP2} [c]	ΔE_{EFP} [d]	species	ΔE_{HF} [b]	ΔE_{EFP} [d]
ATCh(H_2O), gg′, br	23.4	23.3	22.1	23.6	ATCh$(H_2O)_3$, gg′, qa, qa, qa	20.0	21.9
ATCh(H_2O), gg′, qa	17.3	16.9	14.8	16.8	ATCh$(H_2O)_3$, gg′, br, w, qa	27.2	23.5
ATCh(H_2O), gg, br	17.1	17.1	15.3	19.0	ATCh$(H_2O)_3$, gg′, br, br, qa	16.6	13.9
ATCh(H_2O), gg, qa	21.2	20.8	22.5	23.1	ATCh$(H_2O)_3$, gg′, br, br, w	19.1	19.3
ATCh(H_2O), gt, br	20.6	20.4	17.1	19.0	ATCh$(H_2O)_3$, gg′, br, br, br	13.9	10.3
ATCh(H_2O), tg, br	0.0	0.0	0.0	0.0	ATCh$(H_2O)_3$, gg, qa, w, br	17.6	25.1
ATCh(H_2O), tg, qa	5.8	5.4	9.0	7.5	ATCh$(H_2O)_3$, gg, qa, qa, w	17.4	19.2
ATCh(H_2O), tt, br	14.4	14.6	15.9	13.7	ATCh$(H_2O)_3$, gg, qa, qa, br	22.0	23.0
ATCh(H_2O), tt, qa	21.0	20.6	27.9	23.4	ATCh$(H_2O)_3$, gg, qa, qa, qa	19.9	18.9
ATCh$(H_2O)_2$, gg′, qa, qa	20.0	20.1	20.4	18.4	ATCh$(H_2O)_3$, gg, br, w, qa	26.1	25.2
ATCh$(H_2O)_2$, gg′, qa, w	18.0	18.4	18.1	19.6	ATCh$(H_2O)_3$, gg, br, br, qa	10.2	7.9
ATCh$(H_2O)_2$, gg′, br, qa	24.7	24.1	26.0	20.5	ATCh$(H_2O)_3$, gg, br, br, w	13.0	11.1
ATCh$(H_2O)_2$, gg′, br, br	19.4	18.9	16.5	18.8	ATCh$(H_2O)_3$, gg, br, br, br	13.0	13.4
ATCh$(H_2O)_2$, gg′, br, w	28.6	29.9	33.2	28.6			
ATCh$(H_2O)_2$, gg, qa,qa	21.0	21.2	26.7	20.9	ATCh$(H_2O)_3$, gt, qa, qa, w	25.4	28.3
ATCh$(H_2O)_2$, gg, qa, w	18.7	21.2	24.2	22.3			
ATCh$(H_2O)_2$, gg, br, qa	18.7	16.1	21.3	26.6	ATCh$(H_2O)_3$, gt, qa, qa, qa	27.8	27.2
ATCh$(H_2O)_2$, gg, br, br	12.8	12.8	12.2	12.4			
ATCh$(H_2O)_2$, gg, br, w	18.7	20.0	21.3	20.4	ATCh$(H_2O)_3$, gt, br, br, qa	19.3	17.7
ATCh$(H_2O)_2$, gt, qa, qa	28.7	29.3	34.7	28.7	ATCh$(H_2O)_3$, gt, br, br, w	25.1	22.0
ATCh$(H_2O)_2$, gt, qa, w	29.0	28.4	33.5	30.9	ATCh$(H_2O)_3$, gt, br, br, br	18.3	16.3
ATCh$(H_2O)_2$, gt, br, br	22.1	22.2	28.9	22.4	ATCh$(H_2O)_3$, tg, qa, w, br	5.9	12.1
ATCh$(H_2O)_2$, gt, br, w	25.0	26.5	25.4	25.9	ATCh$(H_2O)_3$, tg, qa, qa, w	4.6	5.2
ATCh$(H_2O)_2$, tg, qa, qa	7.7	7.8	15.0	7.8	ATCh$(H_2O)_3$, tg, qa, qa, br	8.1	10.7
ATCh$(H_2O)_2$, tg, qa, w	5.5	5.6	11.1	7.8	ATCh$(H_2O)_3$, tg, qa, qa, qa	10.0	8.5
ATCh$(H_2O)_2$, tg, br, qa	10.0	9.7	14.5	10.4	ATCh$(H_2O)_3$, tg, br, w, qa	2.1	−0.5
ATCh$(H_2O)_2$, tg, br, br	0.0	0.0	0.0	0.0	ATCh$(H_2O)_3$, tg, br, br, qa	−2.2	−2.2
ATCh$(H_2O)_2$, tg, br,w	2.9	4.1	6.7	5.5	ATCh$(H_2O)_3$, tg, br, br, w	0.0	−1.6
ATCh$(H_2O)_2$, tt, qa, qa	21.8	22.2	31.9	21.4	ATCh$(H_2O)_3$, tg, br, br, br	1.4	0.0
ATCh$(H_2O)_2$, tt, qa, w	20.0	20.0	28.8	22.0	ATCh$(H_2O)_3$, tt, qa, w, br	9.9	17.1
ATCh$(H_2O)_2$, tt, br, qa	15.2	14.3	20.1	18.1	ATCh$(H_2O)_3$, tt, qa, qa, w	18.1	20.6
ATCh$(H_2O)_2$, tt, br, w	17.3	18.3	22.9	20.3	ATCh$(H_2O)_3$, tt, qa, qa, br	12.5	13.8
ATCh$(H_2O)_3$, gg′, qa, w, br		20.4		19.0	ATCh$(H_2O)_3$, tt, qa, qa, qa	21.0	19.0
ATCh$(H_2O)_3$, gg′, qa, qa, w		17.4		17.0	ATCh$(H_2O)_3$, tt, br, w, qa	15.8	19.1
ATCh$(H_2O)_3$, gg′, qa, qa, br		16.6		15.0			

[a] HF/6-31G(d)//HF/6-31G(d). [b] HF/6-31G(d)//EFP1/HF/6-31G(d). [c] MP2/6-31G(d)//HF/6-31G(d). [d] EFP1/HF/6-31G(d)//EFP1/HF/6-31G(d).

TABLE 9: HF/6-31G(d) and EFP1/HF/6-31G(d) Hydrogen Bond Lengths and Angles for Several Stable ATCh(H_2O) Structures[a,b]

		$S_7 \cdots H$	angle [c]	$O_9 \cdots H$	angle [c]	$O_{27} \cdots H$	angle [c]
gg, br	EFP1	2.765 (13)	121.2	2.451 (20)	116.6	2.440 (11)	151.0
				2.671 (22)	92.1	2.667 (19)	143.1
				2.498 (28)	123.5	2.451 (20)	152.9
	HF	2.765 (13)	121.2	2.455 (20)	118.0	2.471 (11)	148.9
				2.681 (22)	90.0	2.671 (19)	142.4
				2.285 (28)	134.3	2.352 (20)	155.8
gt, br	EFP1	3.160 (13)	101.7	2.361 (23)	112.3	2.206 (15)	172.0
				2.319 (28)	155.2	2.545 (23)	170.0
	HF	3.155 (13)	101.8	2.376 (23)	111.8	2.194 (15)	171.6
				2.157 (28)	136.9	2.495 (23)	171.0
tg, br	EFP1			2.575 (21)	115.5	2.299 (15)	153.0
				2.519 (23)	96.0	2.603 (18)	142.8
				2.266 (28)	138.2	2.562 (21)	142.9
	HF			2.582 (21)	115.0	2.337 (15)	150.5
				2.518 (23)	96.0	2.575 (18)	142.7
				2.124 (28)	144.0	2.452 (21)	145.4

[a] Hydrogen bonding distances in angstroms and angles in degrees. See Scheme 1 for atom numbering system. Numbers in parentheses indicate hydrogen to which oxygen is hydrogen bonded. [b] Numbering scheme for water molecules: $H_{28}O_{27}H_{29}$. [c] Angle $Y \cdots H-X$ where $Y = S$ or O and $X = C$ or O.

11) and distances between the sulfur and the nitrogen are about 0.4 Å longer than the O···N distances in ACh due to the larger van der Waals radius of sulfur. Therefore, the attractive electrostatic interactions are weaker and the trans form is preferred in ATCh.

The electronic structures can also be analyzed by determining the localized molecular orbitals (LMOs)[68] and then examining O and S lone pairs. If a lone pair is involved in hydrogen bonding or affected by electrostatic interactions, one expects the lone pair LMO to delocalize, and the distance between the LMO centroid and the nuclear center (O or S) should increase. For example, in the water monomer, this distance is 0.580 bohr. However, in the water dimer, the distance between the centroid of the lone pair involved in hydrogen bonding and its O atom increases to 0.610 bohr.

Table 12 lists distances between centroids of LMO lone pairs and O or S centers. Since the tt conformer is least likely to form hydrogen bonds, one may take this rotamer as a reference. Note that the O or S lone pairs in this rotamer are less delocalized than the lone pairs in the H_2O or H_2S (0.979 bohr)

TABLE 10: HF/6-31G(d) and EFP1/HF/6-31G(d) Hydrogen Bond Lengths and Angles for Several Stable ATCh(H_2O)$_2$ Structures[a,b]

		$O_9\cdots H$	angle[c]	$O_{27}\cdots H$	angle[c]	$O_{30}\cdots H$	angle[c]
gg, br,br	EFP1	2.222 (28)	139.7	2.796 (20)	146.6	2.473 (11)	144.7
				1.972 (31)	155.9	2.316 (19)	151.8
						2.596 (20)	144.1
	HF	2.112 (28)	142.2	2.859 (20)	145.4	2.468 (11)	144.9
				1.907 (31)	161.0	2.350 (19)	149.6
						2.479 (20)	147.1
gt, br,br	EFP1	2.162 (28)	147.5	2.810 (23)	135.0	2.452 (13)	145.0
				1.956 (29)	157.1	2.317 (15)	149.5
						2.622 (23)	151.3
	HF	2.072 (28)	151.0	2.790 (23)	137.0	2.449 (13)	147.1
				1.892 (29)	161.3	2.315 (15)	152.3
						2.468 (23)	155.8
tg, br,br	EFP1	2.771 (21)	109.9	2.485 (14)	155.8	2.841 (14)	134.9
		2.446 (23)	90.7	1.986 (30)	150.5	2.255 (17)	154.5
		2.166 (28)	143.8			2.396 (21)	149.9
	HF	2.768 (21)	109.6	2.587 (14)	156.6	2.792 (14)	135.8
		2.442 (23)	99.8	1.922 (30)	156.8	2.259 (17)	154.4
		2.061 (28)	147.8			2.403 (21)	150.4

[a] Hydrogen bonding distances in angstroms and angles in degrees. See Scheme 1 for atom numbering system. Numbers in parentheses indicate hydrogen to which oxygen is hydrogen bonded. [b] Numbering scheme for water molecules: $H_{28}O_{27}H_{29}$ and $H_{31}O_{30}H_{32}$. [c] Angle $O\cdots H-X$ where X = C or O.

TABLE 11: HF/6-31G(d) Mulliken Charges on N, O_7/S_7, and O_9 in ACh and ATCh

ACh

	Mulliken charges		
	N	O_7	O_9
gg′	−0.57	−0.61	−0.57
gg	−0.57	−0.62	−0.54
gt	−0.57	−0.65	−0.52
tg	−0.58	−0.61	−0.57
tt	−0.58	−0.63	−0.53

ATCh

	Mulliken charges		
	N	S_7	O_9
gg′	−0.57	0.18	−0.52
gg	−0.57	0.14	−0.50
gt	−0.58	0.11	−0.47
tg	−0.58	0.20	−0.52
tt	−0.58	0.16	−0.49

TABLE 12: HF/6-31G(d) Localized Molecular Orbital Analysis

species	distance (bohr)[a]		species	distance (bohr)[a]	
ACh, gg′	0.564[b]	0.528	ATCh, gg′	0.953[b]	0.943
ACh, gg	0.545[b]	0.548	ATCh, gg	0.964[b]	0.940
ACh, gt	0.556[b]	0.546	ATCh, gt	0.963[b]	0.940
ACh, tg	0.532[b]	0.548	ATCh, tg	0.952[b]	0.938
ACh, tt	0.534	0.544	ATCh, tt	0.951	0.956

[a] Distance between the centroid of lone pairs and the nuclear center (O or S). [b] The lone pair may be involved in forming hydrogen bonds.

monomers. Relative to tt, the isomers with gauche NCCO are more delocalized, since the LMO centroid in these species (gg′, gg, and gt) are 0.01−0.03 bohr further from the nuclear centers. Similar trends are observed for gauche NCCS in ATCh. However the hydrogen bonding in gauche NCCS is not as strong as in gauche NCCO, since the van der Waals radius of S is much bigger than that of O. Since the internal hydrogen bonds in ACh and ATCh are not as strong as the hydrogen bond in the water dimer, ACh and ATCh are stabilized in aqueous solution by forming bridged hydrogen bonds with water.

V. Conclusions

Both the HF-based effective fragment potential method and fully ab initio HF calculations have been employed in the study of ACh and ATCh hydrated structures, with up to two water molecules. EFP1 geometries are generally in quite good agreement with the much more time-consuming HF results, except for very few noticeable deviations. Relative energies based on EFP1 and HF optimized geometries are mostly within 4 kJ/mol. This difference is within the tolerance of HF theory. Furthermore, both methods preserve the important trends and predict the same low energy structures. These results demonstrate that the HF based EFP1 method can well represent the fully ab initio HF method. Therefore, the calculations of three-water hydrated structures are only performed using the EFP1 method.

Studies of ACh(H_2O)$_n$ show that hydration has only a limited effect on ACh structures as there are only slight changes in the backbone of ACh (except the gg′ conformation). The bridge structure is energetically favored. Similar to structures in the gas phase, it is difficult to find a predominant conformation in solution. Energetically stable bridged structures of several rotamers prefer gauche $N_1C_5C_6O_7$, in analogy with the gas phase.

Five ATCh rotamers, similar to those of ACh, have been identified at the HF/6-31G(d) theory level. This similarity in the backbone structures implies that ATCh and ACh should have similar hydrated structures. However, they do exhibit a difference in the relative energies of the rotamers: ACh exists as a mixture of gg′, gg, and gt rotamers (0.0, 1.8, and 5.7 kJ/mol at the MP2//HF level, respectively) in the gas phase while ATCh is predicted to be a mixture of tg and gg′ (0.0 and 4.9 kJ/mol at the MP2//HF level respectively). Gauche $N_1C_5C_6O_7$ is favored in ACh whereas trans $N_1C_5C_6S_7$ is lower in ATCh. Studies of ATCh(H_2O)$_n$ show similar results to ACh(H_2O)$_n$: solvation has little effect on the ATCh backbone structure, and the bridged structure is generally preferred.

Population analysis implies that electrostatic interactions between the ester O in ACh and the terminal hydrogens in the methyl groups should be stronger than those between the ester S in ATCh and the hydrogens. Localized molecular orbital analysis demonstrates that gauche $N_1C_5C_6O_7$ rotamers have stronger hydrogen bonds than gauche $N_1C_5C_6S_7$ rotamers.

Intramolecular hydrogen bonds are weaker or absent for both trans $N_1C_5C_6O_7$ and $N_1C_5C_6S_7$ rotamers. These observations may be the main reasons that ACh prefers the gauche $N_1C_5C_6O_7$ arrangement whereas ATCh prefers the trans $N_1C_5C_6S_7$ arrangement. The bridged configuration is favored for $A(T)Ch(H_2O)_n$ because it strengthens the interaction between the carbonyl oxygen and the choline moiety compared to the intramolecular hydrogen bonds.

Acknowledgment. The authors gratefully acknowledge the Air Force Office of Scientific Research (AFOSR) for financial support.

Supporting Information Available: Tables S1−S4 giving hydrogen bond lengths and angles of all other ACh and ATCh conformations. This material is available free of charge via the Internet at http://pubs.acs.org.

References and Notes

(1) Wess, J.; Buhl, T.; Lambrecht, G.; Mutschler, E. *Comprehensive Medicinal Chemistry*; Pergamon: Oxford, 1990; Vol. 3.

(2) Deakyne, C. A.; Meot-Ner, M. *J. Am. Chem. Soc.* **1999**, *121*, 1546.

(3) Sussman, J. L.; Harel, M.; Frolow, F.; Oefner, C.; Goldman, A.; Toker, L.; Silman, I. *Science* **1991**, *253*, 871.

(4) Quinn, D. M. *Chem. Rev.* **1987**, *87*, 955.

(5) Sussman, J. L.; Silman, I. *Curr. Opin. Struct. Biol.* **1992**, *2*, 721.

(6) Harel, M.; Quinn, D. M.; Nair, H. K.; Silman, I.; Sussman, J. L. *J. Am. Chem. Soc.* **1996**, *118*, 2340.

(7) Dougherty, D. A.; Stauffer, D. A. *Science* **1990**, *250*, 1558.

(8) Kumpf, R. A.; Dougherty, D. A. *Science* **1993**, *261*, 1708.

(9) Dougherty, D. A. *Science* **1996**, *271*, 163−168.

(10) Canepa, F. G.; Pauling, P.; Sorum, H. *Nature (London)* **1966**, *210*, 907.

(11) Svinnig, T.; Sorum, H. *Acta Crystallogr. Sect. B* **1975**, *31*, 1581.

(12) Jagner, S.; Jensen, B. *Acta Crystallogr. Sect. B* **1977**, *33*, 2757.

(13) Liquori, A. M.; Damiani, A.; De Caen, J. L. *J. Mol. Biol.* **1968**, *33*, 445.

(14) Cushley, R. J.; Mautner, H. G. *Tetrahedon* **1970**, *26*, 2151−2159.

(15) Partington, P.; Feeney, S.; Burgen, A. S. V. *Mol. Pharmacol.* **1972**, *8*, 269−277.

(16) Terui, Y.; Veyama, M.; Satoh, S. *Tetrahedron* **1974**, *30*, 1465.

(17) Lichtenberg, D.; Kroon, P.; Chan, S. *J. Am. Chem. Soc.* **1974**, *96*, 5934.

(18) Cassidei, L.; Sciacovelli, O. *J. Am. Chem. Soc.* **1981**, *103*, 933.

(19) Wilson, J. K.; Derreumaux, P.; Vergoten, G.; Peticolas, W. L. *J. Phys. Chem.* **1989**, *93*, 1351.

(20) Shefter, E.; Kennard, O. *Science* **1966**, *153*, 1389.

(21) Mahajan, V.; Sass, R. L. *J. Cryst. Mol. Struct.* **1974**, *4*, 15.

(22) Marzotto, A.; Gaziani, R.; Bombieri, G.; Forsellini, E. *J. Cryst. Mol. Struct.* **1974**, *4*, 253.

(23) Sax, M.; Rodrigues, M.; Blank, G.; Wood, M. K.; Pletcher, J. *Acta Crystallogr. Sect. B* **1976**, *32*, 1953.

(24) Datta, N.; Mondal, P.; Pauling, P. J. *Acta Crystallogr. Sect. B* **1980**, *36*, 906.

(25) Jensen, B. J. *Acta Crystallogr. Sect. B* **1982**, *38*, 1185.

(26) Jack, J. J.; Hercules, D. M. *Anal. Chem.* **1971**, *43*, 729.

(27) Culvenor, C. C. J.; Ham, N. S. *J. Chem. Soc., Chem. Commun.* **1966**, 537.

(28) Fellman, J. H.; Fujita, T. S. *Nature (London)* **1966**, *211*, 848.

(29) Chothia, C.; Pauling, P. *Nature (London)* **1968**, *219*, 1156.

(30) Egan, M. A.; Zoeller, R. W. *J. Org. Chem.* **1993**, *58*, 1719.

(31) Pullman, B.; Courriere, P.; Coubeils, J. L. *Mol. Pharmacol.* **1971**, *7*, 397.

(32) Weintraub, A. H.; Hopfinger, H. J. *Jerusalem Symp. Quantum Chem. Biochem.* **1974**, *7*, 131.

(33) Beveridge, D. L.; Radna, R. J. J. *J. Am. Chem. Soc.* **1974**, *96*, 3769−3778.

(34) Gelin, B. R.; Karplus, M. J. *J. Am. Chem. Soc.* **1975**, *97*, 6996.

(35) Klimikowski, V. J.; Schafer, L.; Scarsdale, J. N.; Alsenoy, C. U. *J. Mol. Struct.* **1984**, *109*, 311.

(36) Froimowitz, M.; Gans, P. J. *J. Am. Chem. Soc.* **1972**, *94*, 8020.

(37) Genson, D. W.; Christoffersen, R. E. *J. Am. Chem. Soc.* **1973**, *95*, 362.

(38) Port, G. N. J.; Pullman, A. *J. Am. Chem. Soc.* **1973**, *95*, 4059.

(39) Pullman, A.; Port, G. N. J. *J. Theor. Chem.* **1973**, *32*, 77.

(40) Kier, L. B. *Mol. Pharmacol.* **1967**, *3*, 487.

(41) Radna, R. J.; Beveridge, D. L.; Bender, A. L. *J. Am. Chem. Soc.* **1973**, *95*, 3831.

(42) Margheritis, C.; Corongiu, G. *J. Comput. Chem.* **1988**, *9*, 1.

(43) Belcastro, M.; Marino, T.; Mineva, T.; Russo, N.; Sicilia, E.; Toscano, M. In *Recent Development and Applications of Modern Density Functional Theory*; Seminario, J. M., Ed.; Elsevier: Amsterdam; Vol 4, p 743.

(44) Froimowitz, M.; Gans, P. J. *J. Am. Chem. Soc.* **1972**, *94*, 8020.

(45) Edvardsen, O.; Dahl, S. G. *J. Neural Transmission* **1991**, *83*, 157.

(46) Langlet, J.; Claverie, P.; Pullman, B.; Piazzola, D.; Daudey, J. P. *Theor. Chim. Acta* **1977**, *46*, 105.

(47) Pullman, B.; Courriere, P. *Mol. Pharmacol.* **1972**, *8*, 371.

(48) Segall, M. D.; Payne, M. C.; Boyes, R. N. *Mol. Phys.* **1998**, *93*, 365.

(49) Marino, T.; Russo, N.; Tocci, E.; Toscno, M. *Theor. Chem. Acc.* **2001**, *107*, 8.

(50) Kim, Y. J.; Kim, S. C.; Kang, Y. K. *J. Mol. Struct.* **1992**, *269*, 231.

(51) Gelin, B. R.; Karplus, M. *J. Am. Chem. Soc.* **1975**, *97*, 6996.

(52) Vistoli, G.; Pedretti, A.; Villa, L.; Testa, B. *J. Am. Chem. Soc.* **2002**, *124*, 7472.

(53) Barak, D.; Ordentlich, A.; Bromberg, A.; Kronman, C.; Marcus, D.; Lazer, A.; Ariel, N.; Velan, B.; Shafferman, A. *Isr. Biochem.* **1995**, *34*, 15442.

(54) Gordon, M. S.; Freitag, M. A.; Bandyopadhyay, P.; Jensen, J. H.; Kairys, V.; Stevens, W. J. *J. Phys. Chem. A* **2001**, *105*, 293.

(55) Day, P. N.; Jensen, J. H.; Gordon, M. S.; Webb, S. P.; Stevens, W. J.; Krauss, M.; Garmer, D.; Basch, H.; Cohen, D. *J. Chem. Phys.* **1996**, *105*, 1968.

(56) Schmidt, M. W.; Baldridge, K. K.; Boatz, J. A.; Elbert, S. T.; Gordon, M. S.; Jensen, J. H.; Koseki, S.; Matsunaga, N.; Nguyen, K. A.; Su, S.; Windus, T. L.; Dupuis, M.; Montgomery, J. A. *J. Comput. Chem.* **1993**, *14*, 1347.

(57) Bode, B. M.; Gordon, M. S. *J. Mol. Graphics Mod.* **1998**, *16*, 133.

(58) Desiraju, G. R. *Acc. Chem. Res.* **1991**, *24*, 290.

(59) Steiner, T.; Saenger, W. *J. Am. Chem. Soc.* **1992**, *114*, 10146.

(60) Brown, T.; LeMay, H. E., Jr.; Bursten, B. E.; Burdge, J. R. *Chemistry*; 9th Ed.; Pearson Education: Upper Saddle River, NJ, 2003.

(61) Meot-Ner (Mautner), M.; Deakyne, C. A. *J. Am. Chem. Soc.* **1985**, *107*, 469.

(62) Lee, J. Y.; Lee, S. J.; Choi, H. S.; Cho, S. J.; Kim, K. S.; Ha, T. K. *Chem. Phys. Lett.* **1995**, *232*, 67.

(63) Kim, K. S.; Lee, J. Y.; Lee, S. J.; Ha, T. K.; Kim, D. H. *J. Am. Chem. Soc.* **1994**, *116*, 7399.

(64) Pullman, A.; Berthier, G.; Savinelli, R. *J. Am. Chem. Soc.* **1998**, *120*, 8553.

(65) Meot-Ner (Mautner), M.; Sieck, L. W.; Scheiner, S.; Duan, X. *J. Am. Chem. Soc.* **1994**, *116*, 7848.

(66) Meot-Ner (Mautner), M.; Sieck, L. W.; Scheiner, S.; Duan, X. *J. Am. Chem. Soc.* **1999**, *121*, 7625.

(67) Culvenor, C. C. J.; Ham, N. S. *J. Chem. Soc., Chem. Commun.* **1970**, *19*, 1242.

(68) Edmiston, C.; Ruedenberg, K. *Rev. Mod. Phys.* **1963**, *35*, 457.